Application of synthesized copper nanoparticles using aqueous extract of *Ziziphus mauritiana* L. leaves as a colorimetric sensor for the detection of Ag⁺

Roomia MEMON[1] , Ayaz Ali MEMON[1] , Syed Tufail Hussain SHERAZI[1],* , Sirajuddin[2] , Aamna BALOUCH[1] ,
Muhammad Raza SHAH[2] , Sarfaraz Ahmed MAHESAR[1] , Kausar RAJAR[1] , Muhammad Hassan AGHEEM[3]

[1]National Centre of Excellence in Analytical Chemistry, University of Sindh, Jamshoro, Pakistan
[2]International Center for Chemical and Biological Sciences, HEJ Research Institute of Chemistry, University of Karachi, Sindh, Pakistan
[3]Center for Pure and Applied Geology, University of Sindh, Jamshoro, Pakistan

Abstract: The presented work demonstrates the preparation of copper nanoparticles (CuNPs) via aqueous leaves extract of *Ziziphus mauritiana* L. (*Zm*) using hydrazine as a reducing agent. Various parameters such as volume of extract, concentration of hydrazine hydrate, concentration of copper chloride, and pH of the solution were optimized to obtain *Ziziphus mauritiana* L. leaves extract derived copper nanoparticles (*Zm*-CuNPs). Brownish red color was initial indication of the formation of *Zm*-CuNPs while it was confirmed by surface plasmon resonance (SPR) band at wavelength of 584 nm using ultraviolet-visible (UV-vis) spectroscopy. Synthesized *Zm*-CuNPs were characterized by Fourier transform infrared spectroscopy (FT-IR), scanning electron microscopy (SEM), atomic force microscopy (AFM), and X-ray diffractometry (XRD). AFM images showed that the particle size of *Zm*-CuNPs was from 7 to 17 nm with an average size of 11.3 nm. Fabricated sensor (*Zm*-CuNPs) were used as a colorimetric sensor for the detection of Ag⁺ at a linear range between $0.67 \times 10^{-6} – 9.3 \times 10^{-6}$ with R² value of 0.992. For real water samples, limit of quantification (LOQ) and limit of detection (LOD) for Ag⁺ was found to be 330×10^{-9} and 100×10^{-9}, respectively.

Keywords: Copper nanoparticles, *Ziziphus mauritiana* L., plant leaves extract, sensor, silver ion

1. Introduction

Silver (Ag) is a rare, naturally occurring element in the earth. It is considered as one of the more important metals after gold, for the preparation of ornaments. It is widely used in a variety of objects, especially in jewelry and tableware. It has versatile nature and exhibits many industrial and medicinal properties, such as, being a catalyst, used in photography, brazing alloys, electrical conductors, batteries, imaging, silver solder, biomedical, dental alloys, pharmaceutical, and antibacterial activities [1–4]. However, some adverse effects have been reported on the human body due to the use of silver in the dental amalgam, catheters, accidental wounds, and needles [5]. Additionally, high intake of silver may lead to blood pressure, stomach irritation, decreased respiration, and increase in diarrhea [6], whereas, prolonged ingestion of low doses of silver may produce fatty liver and kidney disease [7]. Similarly, argyrosis disease is also caused by long term ingestion of soluble silver compounds, as their small amount accumulates in the brain and muscles. Decrease in mitochondrial functions, organ failure and cytotoxicity may also be due to the chronic exposure of silver ions (Ag⁺) [4]. Therefore, the maximum permitted level of silver in drinking water by Environmental Protection Agency of US is 0.9 μM [5]. Assessment of silver is very important in marine ecosystems for environmental monitoring and public health.[6]. Negative impacts of silver on human health are still controversial and are not very well established [7]. However, it is well known fact that high amounts of silver have adverse effects on aquatic life and are considered as one of the main environmental pollutants [8]. Consequently, determination of Ag⁺ at trace level in water has remained a very important task for many researchers for health and economical reasons. Already, various techniques such as inductive couple plasma mass spectrometric methods (ICP-MS) [9], stripping voltammetry [10], atomic emission and electrochemical methods [11], and stripping and Kelvin force probe microscopic methods [12] have been reportedly used for the detection of silver ion at trace level. But these methods require lengthy sample preparation, hazardous chemicals, sophisticated instruments, and need trained operators. To overcome these issues, optical sensors based on metal nanoclusters for determination of silver ion have been developed due to cost-effectiveness, simple, and quick observation [13]. Colorimetric method for the detection of Ag⁺ at trace level has also been reported by

many researchers [1, 14, 15]. Research is based on continuous improvements. From an economic and an environmental point of view, a favorable method for the synthesis of nanoparticles may include working at room temperature, at neutral pH, and green reducing and capping materials. Generally, plants are considered as natural "chemical factories". It has been confirmed through various studies that the reduction of metals into their respective metals nanoparticles has been carried out through plant extracts containing polyphenols, terpenoids, alkaloids, sugars, proteins, and phenolic acids. A variety of plant extracts have been used for green synthesis of different metal nanoparticles such as cobalt [16], Ag [17], Au [18], Pd [19], ZnO [20], magnetites (Fe and Ni) [21–22], and Cu NPs [23–26]. *Ziziphus mauritiana* L. (*Zm*) is a fruit tree and well known for its medicinal as well as nutritional benefits [27,28]. It is commonly known as Jujube and locally known as 'Ber'. It is a tropical fruit found in many parts of the world including Pakistan, Africa and India. It belongs to the family *Rhamnaceae* [29]. It has multiple medical advantages like antihyperglycemic, antiinflammatory, antiplasmodial, and antimicrobial activities, as well as hemolytic anemia, sedative (tranquilliser), anxiolytic, diuretic, analgesic (pain reliever), and antioxidant properties. The leaves of *Zm* are are also very beneficial to human health and are eaten with catechu as an astringent. They are considered as diaphoretic and especially preferred for typhoid in children [10].

In the current study, the synthesis of CuNPs involves aqueous leaves extract of *Zm* and hydrazine hydrate as a reducing, as well as, an oxygen removing agent. Fabricated copper nanoparticles (CuNPs) were used as a colorimetric sensor for the detection of silver (Ag^+) at trace level in real water samples. As we know, there are the two novel aspects of the current work; it is the first time that *Zm* plant extract has been used for the synthesis of copper nanoparticles, and there are currently no other studies on copper nanoparticles for colorimetric sensing of Ag^+.

2. Experimental

2.1. Chemicals and reagents
In the current study, all chemicals and reagents were of analytical grade and used without any further treatment. Copper chloride ($CuCl_2.2H_2O$), hydrazine monohydrate ($N_2H_4.H_2O$ 99.9%), silver nitrate ($AgNO_3$ 99.9%), potassium nitrate (KNO_3 99.9%), zinc chloride ($ZnCl_2$ 97%), calcium chloride ($CaCl_2$ 97%), cadmium chloride ($CdCl_2$ 98 %), lead chloride ($PbNO_3$ 99.5%), sodium nitrate ($NaNO_3$ 99%), magnesium chloride ($MgCl_2$ 99.9%), hydrochloric acid (HCl 37%), nitric acid (HNO_3 98%), sodium hydroxide pellets (NaOH 99%), and ethanol (C_2H_5OH 97%) were obtained from Sigma-Aldrich Corp. (St. Louis, MO, USA). The preparation of solution was carried out by dissolving a specific amount of each chemical in Milli-Q water (EMD Millipore Corp., Billerica, MA, USA).

2.2. Instrumentation
Ultraviolet-visible (UV-vis) absorption spectra of synthesized *Zm*-CuNPs were recorded on Lambda 356 spectrophotometer (PerkinElmer Inc., Waltham, MA, USA) between 200–800 nm. Interaction between CuNPs and phytochemicals of plant extract was confirmed by FT-IR spectrophotometer (Nicolet 5700 of Thermo Madison, Thermo Electron Scientific Instruments Corp., Madison, WI, USA). Scanning electron microscopy (SEM JSM-6380 LV, JEOL Ltd., Tokyo, Japan) was used to analyze the structural characterization and morphology of prepared *Zm*-CuNPs. To confirm the size and shape of NPs, atomic force microscope (Agilent 5500, Agilent Technologies, Inc. Santa Clara, CA, USA) was used. Crystalline properties of fabricated *Zm*-CuNPs were confirmed by XRD (D-8, Bruker AXS GmbH, Karlsruhe, Germany). Digital camera was used to record visual colorimetric detection of Ag^+ by copper nanoparticles.

2.3. Preparation of plant leaves extract
Fresh leaves (25 g) of *Ziziphus mauritiana* were weighted and added into 100 mL volumetric flask. The solution was boiled at 100 °C for 15 min then cooled at room temperature. Whatman filter paper (No.1) was used for filtration of the extract to get a clear solution. The filtrate was stored at 4 °C for further synthesis of nanoparticles.

2.4. Synthesis protocol of copper nanoparticles
Various parameters, such as, volume of aqueous extract of Zm leaves, volume of reducing agent (1 M hydrazine solution), volume of precursor salt (0.01 M $CuCl_2.2H_2O$), and pH were optimized by UV-vis spectrometer and the data represented in the supplementary file as Figures S1–S4, respectively.

As per optimization study, 1 mL of 0.01 M $CuCl_2.2H_2O$, 0.5 mL of plant extract, and 2 mL of 1 M hydrazine hydrate were added into a 10 mL test tube and filled with Mili-Q water up to the mark at neutral pH. The solution mixture was left at room temperature until it appeared brown in color, which indicated the successful formation of *Zm*-CuNPs. No stirring or heating was involved in the process. UV-vis spectroscopy was used for initial confirmation of the formation and stability of the *Zm*-CuNPs.

2.5. Procedure for colorimetric sensing of silver ion
The colorimetric detection of silver ion was carried out at room temperature. For the development of calibration, known concentration of Ag^+ ranging from 0.67 to 9.3 µM prepared from silver nitrate stock solution (0.1 µM) mixed with 3 mL

of biosynthesized copper nanoparticles solution. After a few minutes the solution was transferred into a 1 cm quartz cell to check colorimetric response. Spectroscopic study was conducted at spectral range from 200 to 800 nm by using Milli-Q water as reference reagent. Change in color from brown to blackish color was considered as a visual check and change in absorbance (delta absorbance) during LSPR study and was used as a quantitative response for the determination of silver in colorimetric system. Color change was observed from brown to blackish with change in absorbance from lower to higher against a blank solution for calibration. The analogous color alterations were also achieved with digital camera after reaction time and it was compared with previously reported detection of silver by other nanoparticles.

2.6. Preparations of real water samples
Different types of water samples such as tape water, surface water, and other sources from different localities were collected, filtered, and diluted to the desired volume. Various concentrations of analyte (Ag^+) were spiked from stock solution (0.1 µM) into 3 mL of Zm-CuNPs. The solutions were kept for 3–4 min at room temperature and then data recorded for each sample in triplicate with the help of UV-vis spectrophotometer.

3. Results and discussion

3.1. UV-visible spectroscopy
In the last few decades, several studies reported that the optical response of metal nanoparticles (NPs) can be adjusted to control size and shape of synthesized nanoparticles [23]. Localized surface plasmon resonance (LSPR) modes of metallic nanoparticles (such as copper, silver, and gold) exist in the visible region of the electromagnetic spectrum. UV/Vis spectroscopy was used for the optimization of different parameters such as precursor salt ($CuCl_2$), reducing agent (hydrazine hydrate), capping agent (leaves extract), and pH for the synthesis of small size CuNPs.

Effect of volume of aqueous extract of *Ziziphus mauritiana* leaves on λ_{max} of CuNPs is shown in Figure S1.

Different volumes ranging from 0.5 to 3 mL of *Ziziphus mauritiana* (*Zm*) leaves extract were used to obtain the optimum volume on the basis of blue shift which indicated smaller size of copper nanoparticles. The best result was achieved by using 0.5 mL of plant extract (*Zm*) at a wavelength of 590 nm by keeping the amount of precursor salt and reducing agent constant. CuNPs have an affinity to oxidize immediately in aqueous medium which is a major negative aspect for using these particles as colorimetric sensors. Hence, to provide an inert environment and to stabilize CuNPs, hydrazine hydrate was used as a reducing agent, which resists the oxidation of CuNPs by evolving nitrogen. Results show the change in LSPR band from 590 nm to a hypsochromic shift of 587 nm by using 1 mL of hydrazine hydrate 0.5–3 mL keeping the constant volume of *Zm* plant extract. The effect of the volume of 1 M hydrazine solution on λ_{max} shift of CuNPs is shown in Figure S2.

Effect of volume of precursor salt (0.01 M $CuCl_2$) ranging from 0.5 to 3 mL solutions is shown in Figure S3. The bathochromic shift and precipitation occurred with bigger particle size using an increased quantity of precursor salt (3 mL). This change in LSPR band may be result of an increased rate of nucleation with greater quantity of copper II ions present in solution. However, 1 mL of precursor salt was selected for further studies.

pH is an important factor for the stability of nanoparticles. Figure S4 shows pH effect on the blue shift, $\lambda_{max,}$ and shape of the peak, which is related to the size of copper nanoparticles in the pH range between 4 and 10.

Furthermore, various factors such as the size of nanoparticles, agglomeration, and nature of capping agents also play important roles in the position, shape, and size of LSPR band. Conversely, protonation/deprotonation of acidic group present in *Zm*-CuNPs might be followed due to change in pH of solution. Substantial changes occurr in shape and width of LSPR band as pH increases from 4 to 10 and pH 7 was selected as optimum pH for *Zm*-CuNPs on the basis of blue shift and shape of SPR band from broad to narrow.

Figure 1 shows UV-visible spectra of synthesized CuNPs with respect to the stability. No significant change was observed in either the color, or in the wavelength of colloidal solution with passage of time. The results show that synthesized *Zm*-CuNPs under optimized parameters were found to be stable for upto 1 month. Therefore, fabricated *Zm*-CuNPs could be used as sensing probe during a wider period and could be stored at room temperature without using special storage conditions.

3.2. Fourier transform infrared spectroscopy
FTIR technique was used to observe interaction between CuNPs and biomolecules of plant extract. Figure 2a shows the FTIR spectrum of plant material and Figure 2b shows the spectrum of *Ziziphus mauritiana* extract capped CuNPs. Bands at 3430.4 cm^{-1}and 3348 cm^{-1}in the FTIR spectrum of the leaves extract are shifted to 3298 cm^{-1} in the FTIR spectrum of *Zm*-CuNPs. Moreover, band at 1729.1 cm^{-1} is due to carbonyl group present in the plant extract (Figure 2a) which has disappeared in FTIR spectrum of *Zm*-CuNPs (Figure 2b). There is also a band at 1618.3 cm^{-1} due to NH bending of
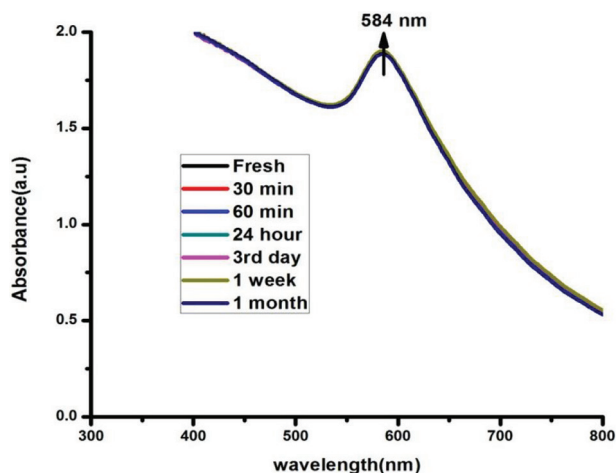
Figure 1. Time based stability of synthesized Zm-CuNPs.
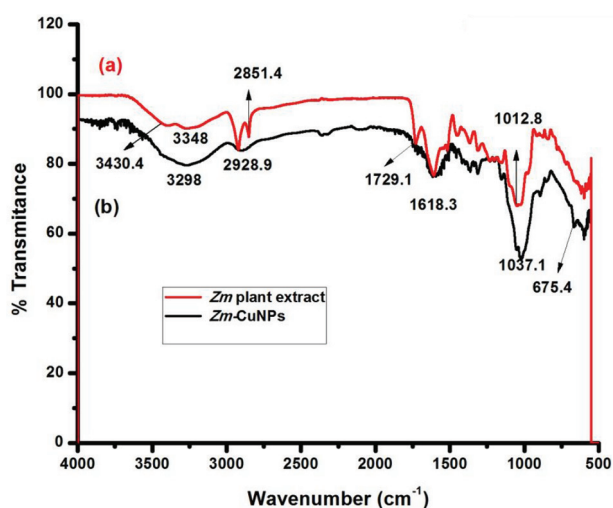

Figure 2. FTIR Spectrum of (a) *Zm* leaves extract (b) *Zm* capped CuNPs.

amide group in both spectra. Also, by comparing the fingerprint region, a new signal at 674.5 cm⁻¹ was observed in FTIR spectrum of *Zm*-CuNPs due to the presence of CuNPs, as it is not present in FTIR spectrum of leaves extract. Therefore, absence of carbonyl band of leave extract and appearance of new peak at 675.5 cm⁻¹ in FTIR spectrum of *Zm*-CuNPs indicated that interaction of biomolecules of leaves extract occurred through carbonyl band with CuNPs.

3.3. Scanning electron microscopy (SEM)
Surface morphology of Zm-CuNPs was studied by SEM image of *Zm*-CuNPs (Figure 3). It was observed that NPs have a rough surface with a spongy, flower like shape. Greater catalytic activity may be due to roughness of surface of *Zm*-CuNPs with larger surface areas [30].

3.4. Atomic force microscopy (AFM)
AFM technique offers visualization and analysis of nanomaterial in three dimensions. As per AFM images (Figure 4a), *Zm*-CuNPs ranged between 7 and 17 nm with an average size of 11.3 nm which was calculated by ImageJ software. Figure 4b shows that size was increased after addition of silver into synthesized *Zm*-CuNPs up to 55 nm. Before sensing *Zm*-CuNPs were monodispersed and spherical in shape as shown in Figure 4a but after the addition of Ag⁺, the morphology and size of *Zm*-CuNPs were totally altered as shown in Figure 4b, may be due to the formation of alloy of Cu and Ag [31]. Figure 4c shows size distribution histogram for *Zm*-CuNPs on the basis of data achieved from AFM.
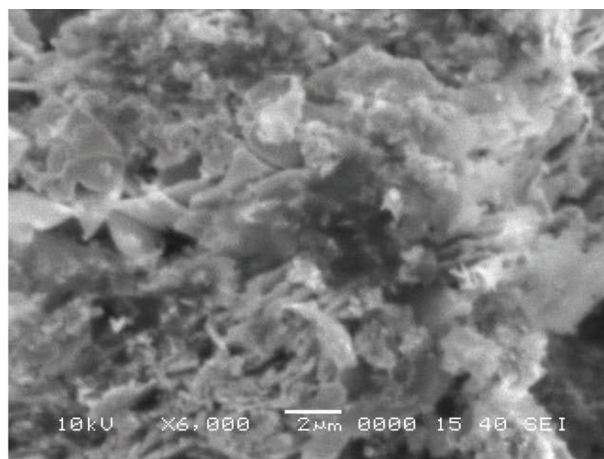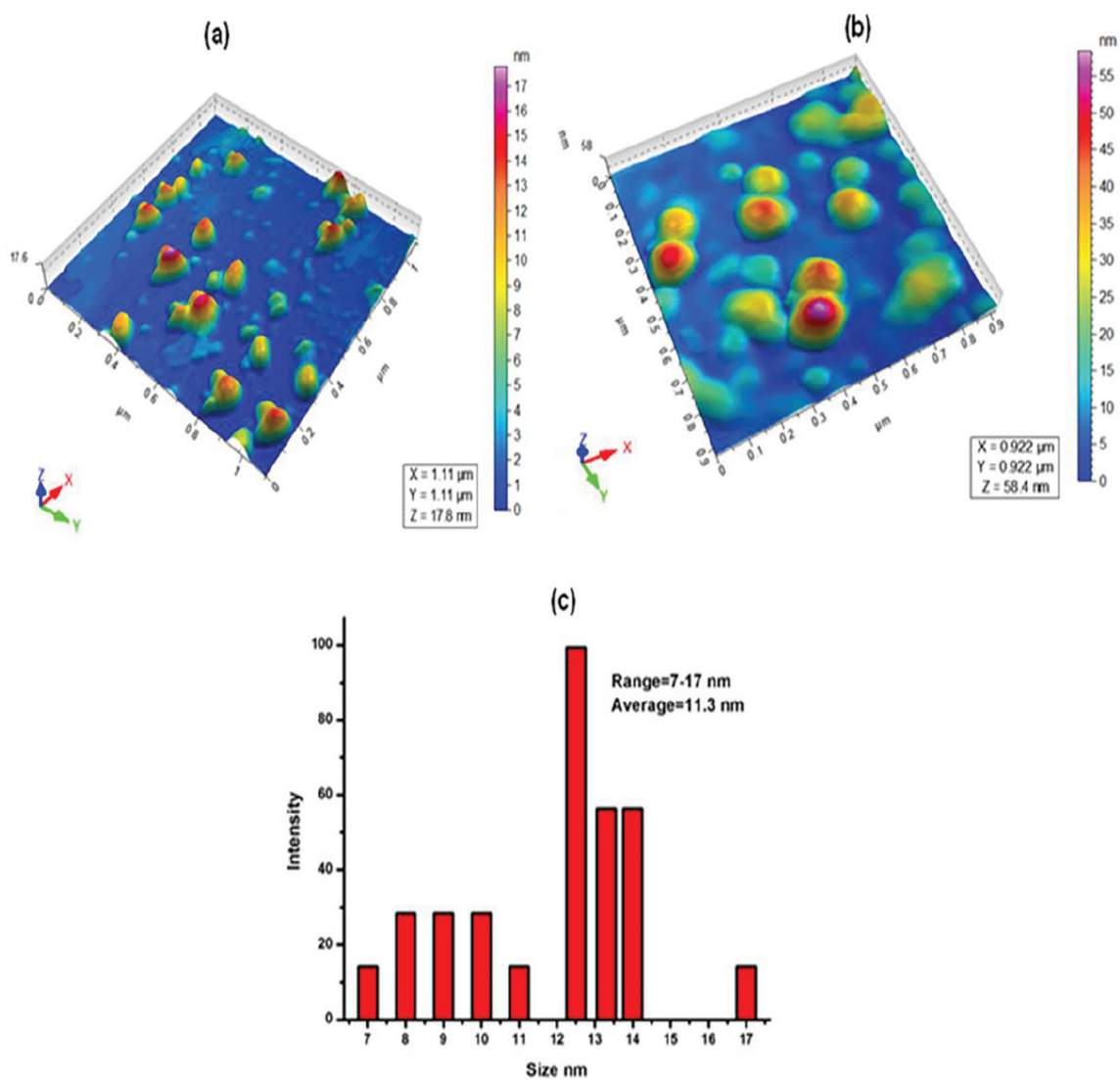
Figure 3. SEM image of Zm-CuNPs.

Figure 4. AFM images of *Zm*-CuNPs (4a) before sensing of Ag$^+$ (4b) after addition of Ag$^+$ (4c) size distribution histogram for *Zm*-CuNPs.

3.5. X-ray diffractometry (XRD)

X-ray powder diffraction (XRD) is a rapid analytical technique basically used for phase recognition of a crystalline material and can provide information on unit cell dimensions. Figure 5 indicates that the diffraction pattern of *Zm*-CuNPs was distinctive face center cubic (FCC) planes of CuNPs at (111),(100), and (220) with high crystalline level at 2θ angles of 31.7°, 45.3°, and 56.4° respectively. These standard planes at particular angles prove that *Zm*-CuNPs are crystalline in nature, verified with the JCPDS data (card no. 89-5899). XRD pattern is comparable with the already reported study [32].

3.6. Colorimetric sensing of Ag$^+$

Figure 6a illustrates colorimetric performance of Zm-CuNPs after the addition of different concentrations of Ag$^+$ in the range between $0.6 \times 10^{-6} – 9.3 \times 10^{-6}$M using UV-vis spectroscopy. Calibration curve showing increase in absorbance with increasing concentration of Ag+ from $0.67–9.3 \times 10^{-6}$ M, inset shows color change with respective addition of Ag+. The color change was observed gradually from brown to blackish after each addition of Ag$^+$. Figure 6b shows the linear plot of added Ag$^+$ concentration in μM versus Δ absorbance. The LOD and LOQ values for Ag$^+$were found to be 100×10^{-9},and 330×10^{-9}M, respectively. LOD was determined as (3*σ)/ slope of linear plot while LOQ was determined as (10*σ)/ slope of linear plot; σ is denoting the standard deviation of at least 3 blank runs measured in Δ absorbance value.

3.7. Selectivity of sensor

Selectivity of colorimetric sensor for Ag+ in the presence of Zn^{2+}, Ni^{2+}, Pb^{2+}, Ca^{2+}, Mg^{2+}, Na$^+$, Cd^{2+}, As^{3+}, and K$^+$ at the concentration of 10 μM was evaluated. The absorption intensity was examined under the same experimental conditions for other metal ions. From Figure 7, it is very clear that no substantial decrease of the absorption signal was observed in the presence of tested interfering ions. The results clearly indicate that there is no significant effect on absorbance and color change of *Zm*-CuNPs solution upon the addition of other tested metal ions, except silver ion which showed distinctive color change with the change in absorbance of surface plasmonic resonance (SPR) band.

3.8. Figures of merit

Comparative results of the currently developed colorimetric sensor with already reported studies [12,14,33–36] are illustrated in Table 1. Although, AuNPs were successfully applied as sensors for the detection of Ag$^+$, the good ranges but the use of Au salts makes these sensors highly expensive. Therefore, developed *Zm*-CuNPs based Ag$^+$ sensor is highly sensitive as LOD is much lower than most of the reported sensors. All the reported colorimetric sensors for the detection of Ag$^+$ are based on AuNPs. According to our best knowledge, our work is the first report of using CuNPs for Ag$^+$ detection. Moreover, *Ziziphus mauritiana* plant extract was used as capping agent which is easily available, cheap, and many active bio-molecules have been already reported in *Ziziphus mauritiana* plant extract [29].

3.9. Comparative studies

Table 2 shows that aqueous extract of different plants has been reported for preparation of various nanoparticles [22,37–44]. In the present study, aqueous leaves extract of *Zm* plant was used as a green material for the synthesis of CuNPs. A small size of Zm-CuNPs ranging from 7 to 17 nm was achieved, compared to reported studies.
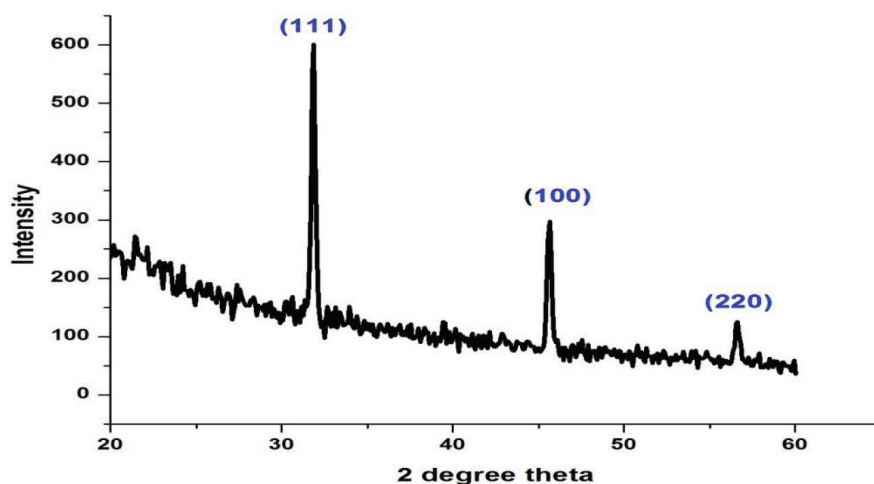

Figure 5. Diffraction patterns of *Zm*-CuNPs with face center cubic planes (FCC) at (111), (100), and (220).
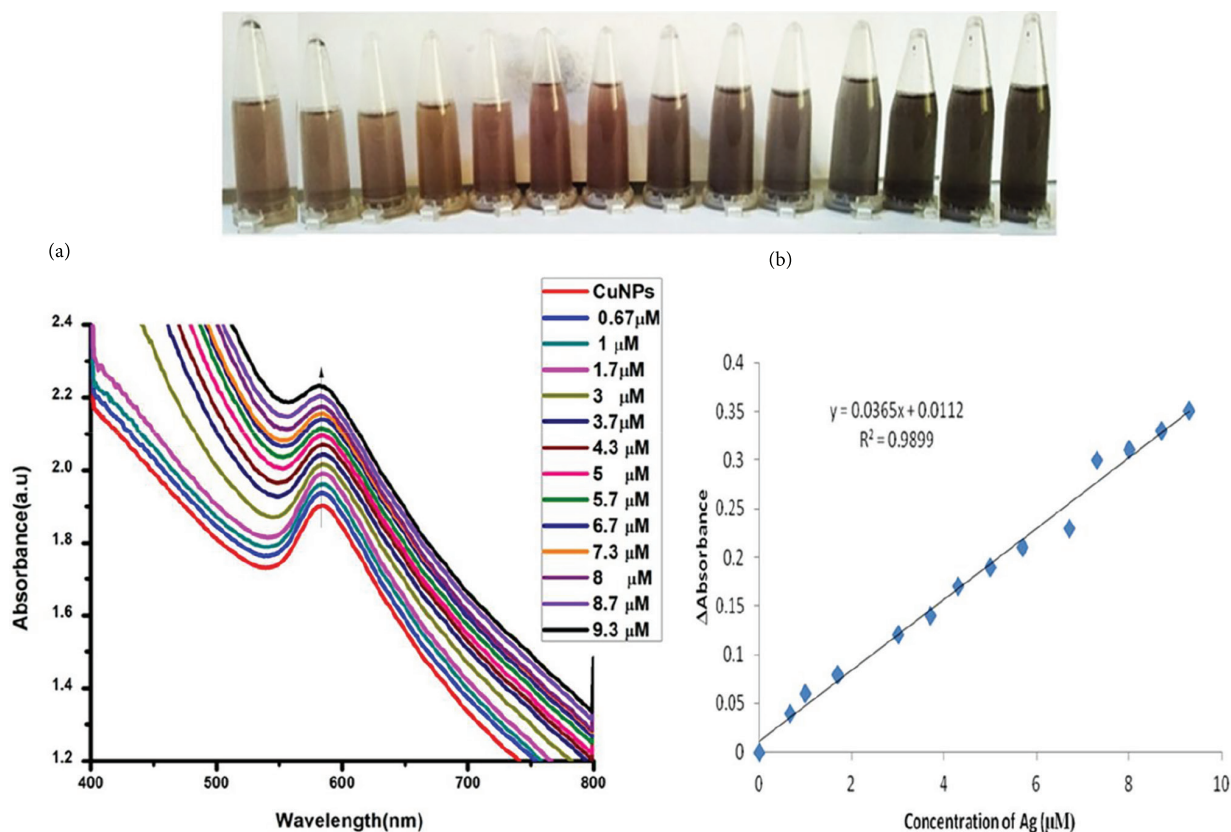
Figure 6. (a) UV-visible spectra of *Zm*-CuNPs with different concentration of Ag$^+$ (0.67–9.3 × 10^{-6} M) while inset shows color change with respective addition of Ag$^+$ (b) Linear regression plot of added concentration of Ag$^+$ (μM) to *Zm*-CuNPs versus change in absorbance (ΔA).
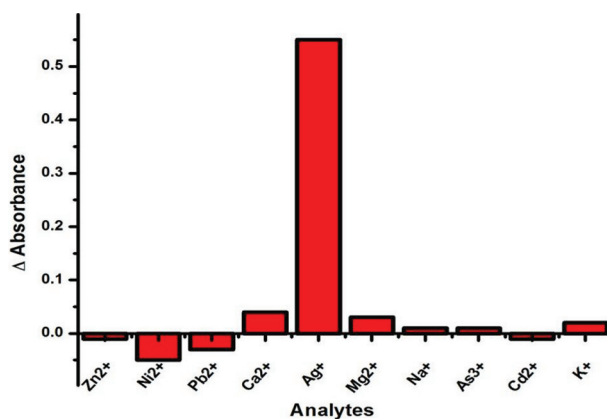

Figure 7. Selectivity of the proposed sensor for Ag+ detection in the presence of possible interfering ions.

3.10. Detection of Ag$^+$ from different real water samples

For practical application of synthesized plant extract based CuNPs sensor, a river water sample was collected from river Indus, Pakistan along with some tape water samples. Ag$^+$ was determined by standards addition method. Six known concentrations of Ag$^+$ (3, 4, and 5 μM in river water and 2, 7, and 9 μM in tape water) were prepared using spiking protocol. The desired volume of each standard was mixed with *Zm*-CuNPs solution and 3 replicate runs were recorded for each analysis. Detection of spiked Ag$^+$ in real water samples with percentage recovery is demonstrated in Table 3. The result

Table 1. Figures of merit of reported and present studies using various metal nanoparticles for detection of Ag$^+$ in water.

Method	Probe	Linear range (M)	LOD (M)	Reference
Colorimetric	BSA@AuNCs	0.5–1 × 10^{-6}	0.204 × 10^{-6}	[14]
Colorimetric	AuNPs	1–9 × 10^{-6}	0.41 × 10^{-6}	[33]
Colorimetric	AuNPs	0.01–1 × 10^{-6}	7.4 × 10^{-6}	[34]
Colorimetric	AuNPs	5–40 × 10^{-6}	1 × 10^{-6}	[35]
Colorimetric	AuNPs	0.1–4 × 10^{-6}	0.05 × 10^{-6}	[12]
Colorimetric	AuNPs	2–28 × 10^{-6}	0.85 × 10^{-6}	[36]
Colorimetric	CuNPs	0.6–9.3 × 10^{-6}	0.1 × 10^{-6}	Current work

Table 2. Different plants used for synthesis of copper nanoparticles by different researchers.

Plant	Precursor salt	Particle size (nm)	Reference
Ocimum sanctum	$CuSO_4$	8–140	[22]
Nerium oleander	$CuSO_4$	40–100	[37]
Punica granatum	$CuCl_2$	40–80	[38]
Eclipta prostrate	$Cu(CH_2COO)_2$	28–45	[39]
Punica tenuiflorum	$CuSO_4$	56–59	[40]
Asparagus adscendens	$CuSO_4$	50–65	[41]
Aloe vera	$CuSO_4$	15–30	[42]
Hemidesmus indicus	$CuSO_4$	26–30	[43]
Allium sativum	$CuSO_4$	83–130	[44]
Ziziphus mauritiana	$CuCl_2$	7–17	Current work

Table 3. Detection of spiked Ag$^+$ in real water samples with percentage recovery.

Samples	Actual (µM)	Spiked (µM)	Found (µM)	SD (±)	% Recovery
S-1	0	3	2.96	0.02	98.6
S-2	0	4	4.10	0.01	102.5
S-3	0	5	4.81	0.01	96.2
Tape water					
S-4	0	2	1.98	0.03	99.0
S-5	0	7	6.90	0.50	98.5
S-6	0	9	8.89	0.01	98.7

revealed that Ag$^+$ in real water sample was successfully detected by *Zm*-CuNPs as a colorimetric sensor with recovery between 96.2 and 102.5%.

4. Conclusion

We conclude that the present work focuses on a new strategy with a greener, cheaper, and facile way of producing highly stable *Zm*-CuNPs using a newer capping agent from *Ziziphus mauritiana* leaves extract. These synthesized nanoparticles are highly stable for up to one month at room temperature and neutral pH (7), without the need of any inert environment. This synthetic strategy is highly economical, more simple, efficient, and less time consuming. Moreover, these stable *Zm*-CuNPs were applied as a sensitive, selective, and economical colorimetric sensor for detection of silver ion at micro molar

level concentration. The best merit of the study lies in the fact that highly stable CuNPs are due to strong capping potential of phytochemicals of plant extract with a small size (11.3 nm), compared to other reported studies.

Acknowledgments

References

1. Wu C, Xiong C, Wang L, Lan C, Ling L. Sensitive and selective localized surface plasmon resonance light scattering sensor for Ag$^+$ with unmodified gold nanoparticles. Analyst 2010; 135: 2682-2687. doi: 10.1039/c0an00201a

2. Sambale F, Wagner S, Stahl F, Khaydarov RR, Scheper T et al. Investigations of the toxic effect of silver nanoparticles on mammalian cell lines. Journal of Nanomaterial 2015; 6: 1-9. doi: 10.1155/2015/136765

3. Drake PL, Hazelwood KJ. Exposure related health effects of silver and silver compounds: a review. The Annals of Occupational Hygiene 2005; 47 (7): 575-585. doi: 10.1093/annhyg/mei019

4. Mijnendonckx K, Leys N, Mahillon J, Silver S, Van Houdt R. Antimicrobial silver: uses, toxicity and potential for resistance. Biometals 2013; 26: 609-621. doi: 10.1007/s10534-013-9645-z

5. Catsakis LH, SulicaVI. Allergy to silver amalgam. Oral Surgery, Oral Medicine, Oral Pathology 1978; 46 (3): 371-375. doi: 10.1016/0030-4220(78)90402-4

6. Panyala NR, Peña-Méndez EM, Havel J. Silver or silver nanoparticles: a hazardous threat to the environment and human health. Journal of Applied Biomedicine 2008; 6: 117-129.

7. Lin YH, Tseng WL. Highly sensitive and selective detection of silver ions and silver nanoparticles in aqueous solution using an oligonucleotide based fluorogenic probe. Chemical Communications 2009; 43: 6619-6621. doi: 10.1039/b915990h

8. Jacobson AR, McBride MB, Baveye P, Steenhuis TS. Environmental factors determining the trace level sorption of silver and thallium to soils. Science of the Total Environment 2005; 345 (1): 191-205. doi: 10.1016/j.scitotenv.2004.10.027

9. Wang YW, Wang M, Wang L, Xu H, Tang S et al. A simple assay for ultrasensitive colorimetric detection of Ag+ at picomolar levels using platinum nanoparticles. Sensors 2017; 17 (11): 2521-2535. doi:10.3390/s17112521

10. Abdallah EM, Elsharkawy ER, Eddra A. Biological activities of methanolic leaf extract of Ziziphus mauritiana. Bioscience Biotechnology Research Communication 2016; 9 (4): 605-614. doi: 10.21786/bbrc/9.4/6

11. Chen Z, Chen B, He M, Wang H, Hu B. A porous organic polymer with magnetic nanoparticles on a chip array for pre-concentration of platinum (IV), gold (III) and bismuth (III) prior to their on-line quantitation by ICP-MS. Microchimica Acta 2019; 186: 107-112. doi: 10.1007/s00604-018-3139-1

12. Park J, Lee S, Jang K, Na S. Ultra-sensitive direct detection of silver ions via kelvin probe force microscopy. Biosensors and Bioelectronics 2014; 60: 299-304. doi: 10.1016/j.bios.2014.04.038

13. Rajar K, Balouch A, Bhanger MI, Shah MT, Shaikh T, Siddiqui S. Succinic acid functionalized silver nanoparticles (Suc-Ag NPs) for colorimetric sensing of melamine. Applied Surface Science 2018; 435: 1080-1086. doi: 10.1016/j.apsusc.2017.11.208

14. Chang Y, Zhang Z, Hao J, Yang W, Tang J. BSA-stabilized Au clusters as peroxidase mimetic for colorimetric detection of Ag+. Sensors and Actuators B: Chemical 2016; 232: 692-697. doi: 10.1016/j.snb.2016.04.039

15. Sung YM, Wu SP. Highly selective and sensitive colorimetric detection of Ag(I) using N-1-(2-mercaptoethyl)adenine functionalized gold nanoparticles. Sensors and Actuators B: Chemical 2014; 197: 172-176. doi: 10.1016/j.snb.2014.02.044

16. Goudarzi M, Salavati-Niasari M. Synthesis, characterization and evaluation of Co_3O_4 nanoparticles toxicological effect; synthesized by cochineal dye via environment friendly approach. Journal of Alloys and Compounds 2019; 784: 676-685. doi: 10.1016/j.jallcom.2019.01

17. Balasubramanian S, Jeyapaul U, Kala SM. Antibacterial activity of silver nanoparticles using Jasminum auriculatum stem extract. International Journal of Nanoscience 2019; 18 (1): 1850011-1850014. doi: 10.1142/s0219581x18500114

18. Philip D. Green synthesis of gold and silver nanoparticles using Hibiscus rosasinensis. Physica E: Low-Dimensional Systems and Nanostructures 2010; 42 (5): 1417-1424. doi: 10.1016/j.physe.2009.11.081

19. Nadagouda MN, Varma RS. Green synthesis of silver and palladium nanoparticles at room temperature using coffee and tea extract. Green Chemistry 2008; 10 (8): 859-862. doi: 10.1039/b804703k

20. Rajar K, Balouch A, Bhanger MI, Sherazi TH, Kumar R. Degradation of 4-Chlorophenol under sunlight using ZnO nanoparticles as catalysts. Journal of Electronic Materials 2018; 47: 2177-2183. doi: 10.1007/s11664-017-6029-0

21. Parveen K, Banse V, Ledwani L. Green synthesis of nanoparticles: their advantages and disadvantages. AIP Conference Proceedings 2016; 1724: 020048-020055. doi: 10.1063/1.4945168

22. Patel BH, Channiwala MZ, Chaudhari SB, Mandot AA. Biosynthesis of coppernanoparticles its characterization and efficacy against human pathogenic bacterium. Journal of Environmental Chemical Engineering 2016; 4: 2163-2169. doi: 10.1016/j.jece.2016.03.046

23. Hussain M, Nafady A, Sherazi ST, Shah MR, Alsalme A et al. Cefuroxime derived copper nanoparticles and their application as a colorimetric sensor for trace level detection of picric acid. RSC Advances 2016; 6: 82882-82889. doi: 10.1039/c6ra08571g

24. Din MI, Rehan R. Synthesis, characterization and applications of copper nanoparticles. Analytical Letters 2017; 50: 50-62. doi: 10.1080/00032719.2016.1172081

25. Valodkar M, Rathore PS, Jadeja RN, Thounaojam M, Devkar RV et al. Cytotoxicity evaluation and antimicrobial studies of starch capped water soluble copper nanoparticles. Journal of Hazardous Materials 2012; 201: 244-249. doi: 10.1016/j.jhazmat.2011.11.077

26. Batoool M, Masood B. Green synthesis of copper nanoparticles using Solanum lycopersicum (tomato aqueous extract) and study characterization. Journal of Nanoscience and Nanotechnology Research 2017; 1 (1): 1-5.

27. Memon A, Memon N, Luthria D, Pitafi A, Bhanger M. Phenolic compounds and seed oil composition of Ziziphus mauritiana L. fruit. Journal of Food and Nutrition Sciences 2012; 62 (1): 15-21. doi: 10.2478/v10222-011-0035-3

28. Memon AA, Memon N, Bhanger MI, Luthria DL. Assay of phenolic compounds from four species of ber (Ziziphus mauritiana L.) fruits: comparison of three base hydrolysis procedures for quantification of total phenolic acids. Food Chemistry 2013; 139 (1-4): 496-502. doi: 10.1016/j.foodchem.2013.01.065

29. Memon AA, Memon N, Bhanger MI, Luthria DL. Phenolic acids composition of fruit extracts of Ber (Ziziphus mauritiana L., var. Golo Lemai). Pakistan Journal of Analytical & Environmental Chemistry 2012; 13 (2): 123-128.

30. Dobrucka R, Kaczmarek M, Dlugaszewska J. Cytotoxic and antimicrobial effect of biosynthesized silver nanoparticles using the fruit extract of Ribes nigrum. Advances in Natural Sciences: Nanoscience and Nanotechnology 2018; 9: 025015-025024. doi: 10.1088/2043-6254/aac5a0

32. Lou T, Chen L, Chen Z, Wang Y, Chen L et al. Colorimetric detection of trace copper ions based on catalytic leaching of silver-coated gold nanoparticles. ACS Applied Materials & Interfaces 2011; 3 (11): 4215-4220. doi: 10.1021/am2008486

33. Safavi A, Ahmadi R, Mohammadpour Z. Colorimetric sensing of silver ion based on anti aggregation of gold nanoparticles. Sensors and Actuators B: Chemical 2017; 242: 609-615. doi: 10.1016/j.snb.2016.11.043

34. He Y, Liang Y, Song H. One-pot preparation of creatinine functionalized gold nanoparticles for colorimetric detection of silver ions. Plasmonics 2016; 11: 587-591. doi: 10.1007/s11468-015-0092-2

35. Li X, Wu Z, Zhou X, Hu J. Colorimetric response of peptide modified gold nanoparticles: an original assay for ultrasensitive silver detection. Biosensors and Bioelectronics 2017; 92: 496-501. doi: 10.1016/j.bios.2016.10.075

36. Du J, Du H, Ge H, Fan J, Peng X. A plasmonicnano-sensor for the fast detection of Ag+ based on synergistic coordination inspired gold nanoparticles Sensors and Actuators B: Chemical 2018; 255: 808-813. doi: 10.1016/j.snb.2017.08.034

37. Gopinath M, Subbaiya R, Selvam MM, Suresh D. Synthesis of copper nanoparticles from Nerium oleander leaf aqueous extract and its antibacterial activity. International Journalof Current Microbiology and Applied Science 2014; 3 (9): 814-818.

38. Padma PN, Banu ST, Kumari SC. Studies on green synthesis of copper nanoparticles using Punica granatum. Annual Research & Review in Biology 2018; 23: 1-10. doi: 10.9734/arrb/2018/38894

39. Chung IM, Abdul Rahuman A, Marimuthu S, Vishnu Kirthi A, Anbarasan K et al. Green synthesis of copper nanoparticles using Ecliptaprostrata leaves extract and their antioxidant and cytotoxic activities. Experimental and Therapeutic Medicine 2017; 14 (1): 18-24. doi: 10.3892/etm.2017.4466

40. Kaur P, Thakur R, Chaudhury A. Biogenesis of copper nanoparticles using peel extract of Punica granatum and their antimicrobial activity against opportunistic pathogens. Green Chemistry Letter Revision 2016; 9 (1): 33-38. doi: 10.1080/17518253.2016.1141238.

41. Thakur SA, Rai RA, Sharma SE. Study the antibacterial activity of copper nanoparticles synthesized using herbal plants leaf extracts. Intentional Journal of Bio-Technology and Research 2014; 4 (5): 21-34.

42. Karimi J, Mohsenzadeh S. Rapid, green, and eco-friendly biosynthesis of copper nanoparticles using flower extract of Aloe vera. Synthesis and Reactivity in Inorganic, Metal Organic and Nano-Metal Chemistry 2015; 45 (6): 895-898. doi: 10.1080/15533174.2013.862644

43. Sivaraj R, Rahman PK, Rajiv P, Narendhran S, Venckatesh R. Biosynthesis and characterization of Acalypha indica mediated copper oxide nanoparticles and evaluation of its antimicrobial and anticancer activity. Spectrochimica Acta Part A: Molecular and Biomolecular Spectroscopy 2014; 129: 255-258. doi: 10.1016/j.saa.2014.03.027

44. Joseph AT, Prakash P, Narvi SS. Phytofabrication and characterization of copper nanoparticles using Allium sativum and its antibacterial activity. International Journal of Science, Engineering and Technology 2016; 4 (2): 463-72.